J. Fluid Mech. (1991), *vol.* 225, *pp.* 153–175
Printed in Great Britain

Trapped modes in open channels

By D. V. EVANS AND C. M. LINTON
School of Mathematics, University of Bristol, Bristol BS8 1TW, UK

(Received 14 May 1990)

Trapped or edge-wave modes are well-known in linear water-wave theory. They occur at discrete frequencies below a certain cutoff frequency and consist of local oscillations trapped near a long horizontal submerged body in finite or infinite depth or over a sloping beach. Less well known is the existence of trapped modes in certain problems in acoustics where the governing equation is the Helmholtz equation. Jones (1953) has proved the existence of such modes which correspond to point-eigenvalues of the spectrum of the differential operator satisfying certain boundary conditions in a semi-infinite region. In this paper we describe a constructive method for determining point-eigenvalues or trapped-mode frequencies in two specific problems in which the two-dimensional Helmholtz equation is satisfied.

The problems arise from a consideration of the fluid motion in a long narrow wave tank with a free water surface which contains a vertical cylinder of uniform horizontal cross-section extending throughout the water depth. Separation of the depth dependence results in Helmholtz's equation with Neumann boundary conditions. By seeking solutions which are antisymmetric with respect to the centreline of the channel, trapped modes are constructed for the case of a cylinder of rectangular cross-section placed symmetrically in the centre of the channel and also for the case of a symmetric rectangular indentation in the tank walls. These problems do not appear to be covered directly by Jones' theory and whilst the method described provides convincing numerical evidence, it falls short of a rigorous existence proof. Extensions to other purely acoustic problems having no water-wave interpretation, including problems which are covered by the general theory of Jones, are also discussed.

1. Introduction

Trapped modes in the linearized theory of surface waves are modes of oscillation at a particular frequency which have finite energy and which persist in some localized region including the free surface whilst decaying rapidly to zero as the free surface extends to infinity. The existence of trapped modes was first established by Ursell (1951) who showed that such a mode could exist in the vicinity of a submerged horizontal circular cylinder with its axis normal to the sides of a deep tank extending to infinity in both directions, provided that the cylinder was sufficiently small. This was not a physical restriction and McIver & Evans (1985) showed numerically that there is always at least one mode above a cylinder of arbitrary size and that further modes are possible as the top of the cylinder approaches the free surface. This was consistent with the general theory of Jones (1953) who proved that trapped modes exist in a tank of finite or infinite depth containing a submerged horizontal cylinder of arbitrary but symmetric cross-section. Recently Ursell (1987) has provided a simplified proof using minimum-energy arguments.

Trapped modes over a submerged horizontal cylinder of rectangular cross-section spanning the bottom of a tank have been obtained by Evans & McIver (1984) who have shown how the trapped-mode frequencies vary with the shelf dimensions and have confirmed bounds on these frequencies which follow from the work of Jones (1953).

Trapped modes can also describe a wave motion in the long-shore direction over an infinitely long submerged cylinder or a variable bottom topography such as a sloping beach or a continental shelf, which decays rapidly to zero in a direction out to sea. In this context they are more commonly referred to as edge waves and are of considerable interest to oceanographers. The simplest such edge wave exists over a uniform sloping beach and was reported by Stokes (1846). He constructed a simple exponential form, vanishing at large distances out to sea but which satisfied the required conditions provided the frequency and long-shore wavenumbers were connected by a simple relation involving the beach slope. Ursell (1952) showed that the Stokes solution was just one of a finite number of edge waves, the number increasing as the beach slope became small. A good description of edge waves in an oceanographic context is given by LeBlond & Mysak (1978).

Trapped modes or edge waves are always associated with a cutoff in the frequency spectrum. For given long-shore wavenumber, there exists a value of the wave frequency above which waves of all frequencies are possible, describing waves obliquely incident upon and scattered by the submerged cylinder or beach. In this range unique reflection and transmission coefficients can be defined at sufficiently large distances away from the cylinder or out to sea. Below the cutoff frequency there exists the possibility of discrete frequencies describing trapped modes which remain local to the cylinder or beach and which do not radiate energy to large distances.

The existence of trapped modes is closely related to the non-uniqueness of a forced-motion problem, since the difference between two solutions of the problem of a long submerged cylinder making small forced harmonic oscillations at a trapped-mode frequency is the trapped mode itself and the usual radiation condition is not sufficient to guarantee uniqueness. Again, if an impulsive motion having a component along its length is given to the cylinder the resulting motion can be described as a Fourier integral over all frequencies. The energy associated with those frequencies above the cutoff frequency will be transferred to large distances away from the cylinder and the ultimate motion will consist of a local oscillation, being a combination of modes at each of the trapped-mode frequencies.

The aim of the present work is to show that trapped modes are not confined to surface-wave problems but can occur quite commonly in acoustic or other problems governed by the Helmholtz equation under certain conditions. Indeed in a very general paper Jones (1953), using the theory of unbounded operators, proves the existence of such modes for the Helmholtz operator in semi-infinite domains satisfying Dirichlet or mixed conditions on the boundaries, and provides bounds for the corresponding point-eigenvalues. As in the case of surface-wave problems, the existence of trapped modes in these acoustic problems requires the presence of a cutoff frequency. The simplest illustration is provided by the solution of $(\nabla^2+k^2)\phi = 0$ in a strip $0 \leqslant y \leqslant d$, $-\infty < x < \infty$, with the so-called 'hard' condition $\phi_y = 0$ on $y = d$ and either a 'hard' or 'soft' condition $\phi = 0$ on $y = 0$. In the former hard–hard case, separation of variables provides solutions $\exp(\pm ikx)$ and $\exp(\pm k_n x)\cos n\pi(d-y)/d$ $(n = 1,2,\ldots)$ where $k_n = (n^2\pi^2/d^2-k^2)^{\frac{1}{2}}$, whilst in the latter hard–soft case, possible solutions are $\exp(\pm\kappa_n x)\sin(n-\frac{1}{2})\pi y/d$ $(n = 1,2,\ldots)$ where $\kappa_n = ((n-\frac{1}{2})^2\pi^2/d^2-k^2)^{\frac{1}{2}}$. It is clear that in the former case wave propagation is always possible for all values of k, whereas in the latter, if $k < \pi/2d$, wave propagation is impossible, the only solution being either exponentially large or small. Thus solutions satisfying the condition $\phi = 0$ on $y = 0$, equivalent to antisymmetric solutions, odd in y, in a strip of width $2d$ exhibit a lowest cutoff frequency, $\omega_c = k_c v$ in the acoustic context, where v is the velocity of sound and $k_c = \pi/2d$. For $\omega < \omega_c$ no waves can propagate. However, it should be noted that a cutoff frequency may exist in waveguides when a hard condition $\phi_n = 0$ is imposed on the boundaries if the cross-section of the guide is variable. See for example Razavy (1989).

We can equally well interpret the above problem as the antisymmetric sloshing of a liquid of depth H contained in the wave tank $-\infty < x < \infty$, $|y| < d$, $-H \leqslant z \leqslant 0$ and we shall concentrate on this water-wave interpretation in most of what follows.

The depth variation $\cosh k(H+z)$ can be separated out leaving the Helmholtz equation and the required relation $\omega^2 = gk \tanh kH$ between k and the wave frequency in order to satisfy the usual linearized free-surface condition for water waves. In this context the lowest cutoff frequency is $\omega_c = (gk_c \tanh k_c H)^{\frac{1}{2}}$ with $k_c = \pi/2d$ as before. Solutions in the tank having bounded total energy, which decay rapidly as $|x| \rightarrow \infty$, are not possible for $k < k_c$ but we shall show that the introduction throughout the water depth of a rectangular block occupying $|x| = a$, $|y| = b < d$, satisfying a no-flow or hard condition on its sides and having two sides parallel to the tank walls but only partially spanning the width of the tank, permits the construction of such trapped-mode solutions antisymmetric about the centreplane of the tank, $y = 0$, with $k < k_c$.

This particular problem, satisfying both hard and soft conditions on different boundaries, does not appear to be covered by the general theory of Jones as it stands, so that the existence of trapped modes is not yet proved in this case. However, the method of construction used in the present work, while falling short of a rigorous proof of the existence of the trapped modes, provides a clear criterion as to when to expect such modes in this class of problem, and how to compute them.

The problem is formulated in §2 using matched eigenfunction expansions to derive a homogeneous integral equation for the horizontal fluid velocity $U(y)$ across the line joining the finite and infinite regions. This is converted by Fourier expansions into a homogeneous infinite system of equations, the vanishing of the determinant of which provides trapped-mode eigenvalues if they exist. See equation (5.1). But by subtracting off the oscillatory part of the kernel of the integral equation corresponding to the lowest eigenvalue in the finite region this is converted into an *in*homogeneous infinite system for unknowns u_n ($n = 0, 1, \ldots$) for which the infinite matrix $\boldsymbol{K}$ is now positive definite, as in equation (2.43). The trapped modes are now determined from equation (2.44), namely $u_0 = \tan ka$. Since $\boldsymbol{K}$ is symmetric and positive definite any $N \times N$ truncation gives a unique (positive) u_n and the positions of the trapped-mode frequencies are easily located as the intersections of u_0 and $\tan ka$, as in equation (2.44).

Considerable care is needed in the numerical work to achieve convergence. This is not surprising since in order to model the singularity in the velocity at the corner of the block we expect the Fourier coefficients of velocity, u_n or U_n, to be $O(n^{-\frac{2}{3}})$ which implies $\sum |U_n|$ does not converge. Also the condition $\sum_m \sum_n |A_{mn}| < \infty$, being sufficient to ensure that $\det(\boldsymbol{I}^{(N)} + \boldsymbol{A}^{(N)}) \rightarrow \det(\boldsymbol{I} + \boldsymbol{A})$ uniformly as $N \rightarrow \infty$ is not satisfied for this problem.

It is found that trapped modes antisymmetric about the vertical centreplane of the wave tank, and either symmetric or antisymmetric about the vertical plane through the middle of the block normal to the tank sides can be constructed for discrete values of $k < k_c$ and for all values of a, and $0 \leqslant b < d$. In §3 trapped modes are shown to exist in a different problem. The block is removed and a symmetric indentation $|y| = b$, $d < b < 3d$, $|x| < a$ is introduced on which a no-flow condition is imposed. Here too trapped modes can be computed for all a, b although again no rigorous existence proof is available. It would appear that no such modes exist if $b < d$, corresponding to a symmetric protrusion from the tank walls.

A number of limiting cases are considered in §4 including explicit equations for the determination of the trapped-mode frequencies in the separate cases $a/d \to 0$ or $b/d \to 1$ when $k \to k_c$. The case $a/d \gg 1$ for the block is related to a reflection problem for a semi-infinite block in a tank, which for $b = 0$ can be solved exactly using the Wiener–Hopf technique (Noble 1958).

Results of numerical computations are given in §5 where a comparison of the various approximations is made, and figures describing the variation of the discrete values of kd corresponding to the trapped modes with a/d, b/d are presented.

Finally in §6 we discuss the possibility of trapped acoustic waves in a variety of other problems in which different boundary conditions are satisfied. This includes the indentation problem with a soft condition on all boundaries, a case where the theory of Jones applies. It is confirmed that the trapped modes constructed by the present method are consistent with the bounds predicted by Jones.

2. Formulation

Cartesian coordinates are chosen with the (x, y)-plane in the undisturbed free surface and z vertically upwards. The sides of the channel are $|y| = d$, $-\infty < x < \infty$ and the water is of depth H. A rectangular block is placed symmetrically in the channel occupying the region $|x| \leqslant a$, $|y| \leqslant b < d$, $-H \leqslant z \leqslant 0$ so that it extends throughout the depth of the fluid. The usual linearized water-wave equations governing the motion of the fluid can be described by a velocity potential $\Phi(x, y, z, t)$ which, assuming simple harmonic motion of radian frequency ω, and because the block extends throughout the entire depth, can be written

$$\Phi(x, y, z, t) = \mathrm{Re}\{\phi(x, y) \cosh k(z+H)\, \mathrm{e}^{-\mathrm{i}\omega t}\}. \tag{2.1}$$

Here k is the unique positive root of

$$\omega^2 = gk \tanh kH \tag{2.2}$$

and $\phi(x, y)$ satisfies

$$(\nabla^2 + k^2)\phi = 0 \quad \text{in the fluid,} \tag{2.3}$$

$$\phi_y = 0, \quad |y| = d, \ -\infty < x < \infty, \tag{2.4}$$

$$\phi_y = 0, \quad |y| = b, \ |x| \leqslant a, \tag{2.5}$$

$$\phi_x = 0, \quad |x| = a, \ |y| \leqslant b, \tag{2.6}$$

$$\phi \to 0, \quad |x| \to \infty, \ |y| \leqslant d, \tag{2.7}$$

and finally, in the light of the discussion in the introduction,

$$\phi = 0, \quad y = 0, \ |x| \geqslant a. \tag{2.8}$$

We seek non-trivial solutions ϕ of (2.3)–(2.8) for certain discrete values of k corresponding to trapped modes with frequency given by (2.2).

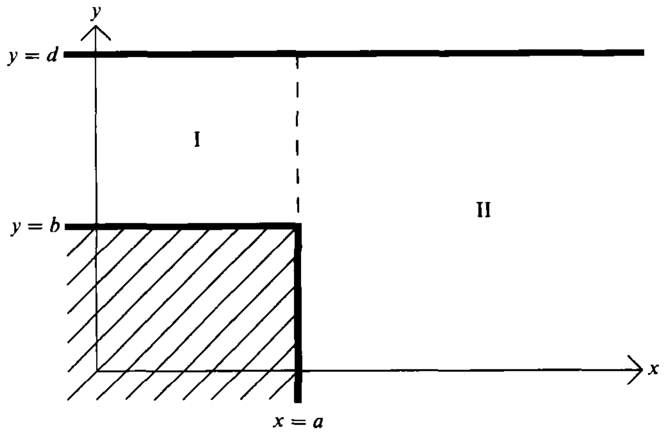

FIGURE 1. Definition sketch.

The above equations also describe a two-dimensional problem in acoustics involving a rectangular obstruction in a wave guide. In this interpretation we are seeking trapped acoustic waves with frequency given by $\omega = kv$, where v is the sound speed.

Two distinct types of solution will be sought, the first ϕ^s symmetric about $x = 0$, the second ϕ^a antisymmetric about $x = 0$. Thus

$$\phi^s(x, y) = \phi^s(-x, y) \tag{2.9}$$

and

$$\phi^a(x, y) = -\phi^a(-x, y). \tag{2.10}$$

The symmetry of the problem permits us to consider only $x \geqslant 0$ and use (2.9) and (2.10) to extend our functions into negative x. The condition (2.8) also permits us to restrict consideration to $0 \leqslant y \leqslant d$ and to extend our functions $\phi^{s,a}$ into $-d \leqslant y \leqslant 0$ using the identity

$$\phi^{s,a}(x, y) = -\phi^{s,a}(x, -y). \tag{2.11}$$

We shall only deal with ϕ^s in detail, since the method for ϕ^a follows similar lines with only minor changes. Thus $\phi^s(x, y)$ satisfies

$$(\nabla^2 + k^2)\,\phi^s(x, y) = 0 \quad \text{in the fluid}, \tag{2.12}$$

$$\phi^s_y = 0, \quad y = d, x \geqslant 0, \tag{2.13}$$

$$\phi^s_y = 0, \quad y = b, 0 \leqslant x \leqslant a, \tag{2.14}$$

$$\phi^s_x = 0, \quad x = a, 0 \leqslant y \leqslant b, \tag{2.15}$$

$$\phi^s \to 0, \quad x \to \infty, 0 \leqslant y \leqslant d, \tag{2.16}$$

$$\phi^s = 0, \quad y = 0, x \geqslant a, \tag{2.17}$$

and

$$\phi^s_x = 0, \quad x = 0, b \leqslant y \leqslant d. \tag{2.18}$$

The geometry of the problem is shown in figure 1. We denote $b \leqslant y \leqslant d$, $0 \leqslant x \leqslant a$ by region I, $x \geqslant a$, $0 \leqslant y \leqslant d$ by region II, and their common boundary, $b \leqslant y \leqslant d$, $x = a$, by L.

We can construct complete orthonormal eigenfunctions $\psi_n(y)$, $\Psi_n(y)$ appropriate to region I, II respectively. Thus the set of functions

$$\psi_n(y) = (\epsilon_n/c)^{\frac{1}{2}} \cos p_n(d-y), \quad n = 0, 1, 2, \ldots, \tag{2.19}$$

where $p_n = n\pi/c$, $c = d-b$, and $\epsilon_n = 2$ if $n \geqslant 1$, $\epsilon_0 = 1$ satisfies

$$\int_L \psi_n(y)\, \psi_m(y)\, \mathrm{d}y = \delta_{mn}$$

whilst the set

$$\Psi_n(y) = (2/d)^{\frac{1}{2}} \sin l_n y, \quad n = 1, 2, \ldots, \tag{2.20}$$

where $l_n = (n-\frac{1}{2})\pi/d$ satisfies

$$\int_0^d \Psi_n(y)\, \Psi_m(y)\, \mathrm{d}y = \delta_{mn}.$$

For later reference we define

$$\int_L \psi_n(y)\, \Psi_m(y)\, \mathrm{d}y = c_{nm}. \tag{2.21}$$

We shall construct general separation-of-variables solutions in each of the two regions and match these solutions and their x-derivatives across the common boundary L. This ensures that both pressure and velocity are continuous on L.

In region I we write

$$\phi^{\mathrm{s}}(x, y) = \sum_{n=0}^{\infty} U_n^{(1)} \frac{\cosh k_n x}{k_n \sinh k_n a} \psi_n(y), \tag{2.22}$$

where
$$k_n = (p_n^2 - k^2)^{\frac{1}{2}}, \quad n \geqslant 1, \quad k_0 = \mathrm{i}k, \tag{2.23}$$

which satisfies (2.12), (2.13) for $0 \leqslant x \leqslant a$, (2.14) and (2.18). Note that since $k < \pi/2d$, k_n is never zero. In region II we write

$$\phi^{\mathrm{s}}(x, y) = \sum_{n=1}^{\infty} U_n^{(2)} (-\kappa_n)^{-1} \mathrm{e}^{-\kappa_n (x-a)}\, \Psi_n(y), \tag{2.24}$$

where
$$\kappa_n = (l_n^2 - k^2)^{\frac{1}{2}}, \tag{2.25}$$

which satisfies (2.12), (2.13) for $x \geqslant a$, (2.16) and (2.17).

The constants $U_n^{(1)}$, $U_n^{(2)}$ are to be determined, to within an arbitrary multiplicative factor, through the matching across L.

Thus the x-component of velocity on $x = a$ is, from (2.22) and (2.24),

$$U(y) = \sum_{n=1}^{\infty} U_n^{(2)}\, \Psi_n(y) = \begin{cases} \sum\limits_{n=0}^{\infty} U_n^{(1)}\, \psi_n(y), & y \in L \\ 0, & 0 \leqslant y \leqslant b. \end{cases} \tag{2.26}$$

If we now multiply (2.26) by $\Psi_m(y)$ and integrate over $[0, d]$ we obtain

$$U_m^{(2)} = \sum_{n=0}^{\infty} U_n^{(1)} c_{nm}, \quad m = 1, 2, \tag{2.27}$$

using (2.21). Notice that condition (2.15) has been applied in deriving (2.27).

Continuity of ϕ^{s} across L now requires

$$\sum_{n=0}^{\infty} U_n^{(1)} k_n^{-1} \coth(k_n a)\, \psi_n(y) = \sum_{n=1}^{\infty} U_n^{(2)} (-\kappa_n)^{-1}\, \Psi_n(y), \quad y \in L. \tag{2.28}$$

We now multiply (2.28) by $\psi_m(y)$ and integrate over L to obtain

$$U_m^{(1)} k_m^{-1} \coth k_m a + \sum_{n=1}^{\infty} U_n^{(2)} \kappa_n^{-1} c_{mn} = 0, \quad m = 0, 1, 2 \ldots. \tag{2.29}$$

If we now substitute for $U_n^{(2)}$ from (2.27) into (2.29) we obtain

$$U_m^{(1)} + \sum_{n=0}^{\infty} A_{mn} U_n^{(1)} = 0, \quad m = 0, 1, 2, \ldots, \tag{2.30}$$

where
$$A_{mn} = k_m \tanh(k_m a) \sum_{r=1}^{\infty} \frac{c_{mr} c_{nr}}{\kappa_r}. \tag{2.31}$$

Alternatively we can substitute for $U_m^{(1)}$ from (2.29) into (2.27) to obtain

$$U_m^{(2)} + \sum_{n=1}^{\infty} B_{mn} U_n^{(2)} = 0, \quad m = 1, 2, \ldots, \tag{2.32}$$

where
$$B_{mn} = \kappa_n^{-1} \sum_{r=0}^{\infty} k_r \tanh(k_r a) c_{rm} c_{rn}. \tag{2.33}$$

Either (2.30) or (2.32) can be used to seek values of kd, for given block dimensions a/d, b/d, for which non-trivial solutions $U_n^{(1)}$ or $U_n^{(2)}$ exist. Details of the numerical procedure used are given in §5.

It is not at all clear from (2.30) or (2.32) that there will be such a solution. However a simple one-term approximation to (2.30) gives, since $k_0 = \mathrm{i}k$,

$$1 = k \tan(ka) \sum_{r=1}^{\infty} \frac{c_{0r}^2}{\kappa_r} \tag{2.34}$$

as the condition for a trapped mode. Since c_{0r} and κ_r are independent of a (2.34) shows that, to this approximation at least, an infinity of solutions must exist for sufficiently large a.

To gain greater insight into possible solutions we proceed as follows. From (2.26) we have

$$U_n^{(1)} = \int_L U(y) \psi_n(y) \, \mathrm{d}y, \quad n = 0, 1, 2, \ldots, \tag{2.35}$$

$$U_n^{(2)} = \int_L U(y) \Psi_n(y) \, \mathrm{d}y, \quad n = 1, 2, \ldots. \tag{2.36}$$

Substitution into (2.28) now gives

$$\int_L U(y') \left\{ \sum_{n=0}^{\infty} k_n^{-1} \coth(k_n a) \psi_n(y) \psi_n(y') + \sum_{n=1}^{\infty} \kappa_n^{-1} \Psi_n(y) \Psi_n(y') \right\} \mathrm{d}y' = 0, \quad y \in L, \tag{2.37}$$

a homogeneous integral equation for $U(y)$. We shift the oscillatory first term in the first summation to the right-hand side of the equation and define

$$U(y) = U_0^{(1)} \cot(ka) u(y), \tag{2.38}$$

whence
$$\int_L u(y')K(y,y')\,\mathrm{d}y' = \psi_0(y), \quad y \in L \tag{2.39}$$

and
$$\int_L u(y)\,\psi_0(y)\,\mathrm{d}y = \tan ka, \tag{2.40}$$

from (2.35) with $n = 0$, where

$$K(y,y') = \sum_{n=1}^{\infty} \{kk_n^{-1}\coth(k_n a)\,\psi_n(y)\,\psi_n(y') + k\kappa_n^{-1}\,\Psi_n(y)\,\Psi_n(y')\}. \tag{2.41}$$

We have replaced our homogeneous infinite system of equations by an inhomogeneous integral equation of the first kind, which in turn can be converted into an inhomogeneous infinite system by expanding $u(y)$ in terms of the complete set $\{\psi_n\}$, $(n = 0, 1, \ldots)$.

We write

$$u(y) = \sum_{n=0}^{\infty} u_n\,\psi_n(y), \tag{2.42}$$

substitute in (2.39), multiply by $\psi_m(y)$ and integrate over L to obtain

$$\sum_{n=0}^{\infty} K_{mn}\,u_n = \delta_{0m}, \quad m = 0, 1, 2, \ldots, \tag{2.43}$$

$$u_0 = \tan ka, \tag{2.44}$$

where
$$\begin{aligned} K_{mn} &= \int_L \psi_m(y) \int_L \psi_n(y')\,K(y,y')\,\mathrm{d}y'\,\mathrm{d}y \\ &= \sum_{r=1}^{\infty} \{kk_r^{-1}\coth(k_r a)\,\delta_{mr}\,\delta_{nr} + k\kappa_r^{-1}\,c_{mr}\,c_{nr}\}. \end{aligned} \tag{2.45}$$

This formulation can also be obtained directly from (2.30), (2.31) but the above derivation is more illuminating. We could also obtain an equivalent formulation starting from (2.32) and (2.33) but since there is no oscillatory term in the outer region this turns out to be more complicated. We shall discuss the merits of these various formulations again when we consider the indentation problem in the next section.

The sum in (2.45) can be shown to converge for any fixed m, n and the positive definite nature of K_{mn} follows from the result

$$\begin{aligned} \sum_{r=1}^{\infty} \left\{kk_r^{-1}\coth(k_r a)\,u_r^2 + k\kappa_r^{-1}\left(\sum_{n=0}^{\infty} c_{nr}\,u_n\right)^2\right\} &= \sum_{m=0}^{\infty}\sum_{n=0}^{\infty} K_{mn}\,u_m\,u_n \\ &= \sum_{m=0}^{\infty} u_m\,\delta_{0m} = u_0 > 0. \end{aligned} \tag{2.46}$$

Thus any Nth-order truncation of the infinite system (2.43) will have a unique solution $u_n^{(N)}$ since $\det K_{mn}^{(N)} \neq 0$, and furthermore $u_0^{(N)} > 0$. The trapped-mode frequencies are now determined by solving $u_0^{(N)} = \tan ka$ for values of N such that $u_0^{(N)}$ remains unchanged, within a desired accuracy, for further increases in N. It is clear from this that there must be a trapped mode in each interval $m\pi < ka < (m+\frac{1}{2})\pi$, $m = 0, 1, 2, \ldots$ for a/d large enough that the intersection point is below the cutoff frequency.

The solution $\phi^a(x,y)$ is derived similarly and is obtained by interchanging the hyperbolic functions in (2.22), replacing the coth in (2.28), (2.29), (2.41) and (2.45) by tanh, the tanh in (2.31), (2.33) by coth, and the tan in (2.34), (2.40), (2.44) by $-\cot$.

3. Trapped waves near an indentation

If the same approach is tried with a rectangular protrusion from the wall of size c, so that fluid region I is $0 \leqslant x \leqslant a$, $0 \leqslant y \leqslant b$, it is found that the matrix equivalent to A_{mn} in (2.31) is positive definite and no non-trivial trapped mode solution is possible. This is because the lowest mode in region I is now proportional to $\cosh k_0 x \sin p_0 y$ where $k_0 = (p_0^2-k^2)^{\frac{1}{2}}$ and $p_0 = \pi/2b$, and for a trapped mode we require $k > p_0$, which contradicts the requirement $k < \pi/2d\,(=l_1)$ arising from the decaying modes in region II.

This suggests that if $b > d$, corresponding to an *indentation* in the wall of depth $b-d$, trapped solutions odd in y should be possible with $p_0 < k < l_1$. Thus region I is now $0 \leqslant x \leqslant a$, $0 \leqslant y \leqslant b$ with $b/d > 1$ whilst region II is as before.

We can construct a solution even in x in region I exactly corresponding to (2.22) provided that in this case we replace ψ by ψ' where

$$\psi'_n(y) = (2/b)^{\frac{1}{2}} \sin p_n y, \quad n = 0,1,2,\ldots, \tag{3.1}$$

where now $p_n = (n+\frac{1}{2})\pi/b$. Also $k_n = (p_n^2-k^2)^{\frac{1}{2}}$, $n \geqslant 1$ as before, but now $k_0 = \mathrm{i}k'$ with $k' = (k^2-p_0^2)^{\frac{1}{2}}$. Note that if $b/d > 3$, k_1 is also imaginary, and in general, if $b/d > 2n+1$, $k_0, k_1, \ldots, k_n$ are all imaginary. In order to keep the analysis as simple as possible we shall restrict our attention to $1 < b/d < 3$.

The solution in region II is the same as (2.24) and continuity of the x-component of velocity, $U(y)$, across $L': 0 \leqslant y \leqslant d$ gives

$$U(y) = \sum_{n=0}^{\infty} U_n^{(1)} \psi'_n(y) = \begin{cases} \sum_{n=1}^{\infty} U_n^{(2)} \Psi_n(y), & y \in L' \\ 0, & d \leqslant y \leqslant b. \end{cases} \tag{3.2}$$

Notice that since region I is now the wider region the expansion of $U(y)$ is now in terms of the set $\{\psi'_n(y)\}$ rather than $\{\Psi_n(y)\}$.

For $y \in L'$

$$\psi'_n(y) = \sum_{m=1}^{\infty} d_{nm} \Psi_m(y), \quad n = 0,1,2,\ldots, \tag{3.3}$$

with d_{nm} given by (2.21) with ψ_n and L replaced by ψ'_n and L' respectively. Thus from (3.2)

$$U_m^{(1)} = \sum_{n=1}^{\infty} U_n^{(2)} d_{mn}, \quad m = 0,1,2,\ldots. \tag{3.4}$$

Continuity of ϕ across L' gives

$$\sum_{n=0}^{\infty} U_n^{(1)} k_n^{-1} \coth(k_n a)\, \psi'_n(y) = \sum_{n=1}^{\infty} U_n^{(2)} (-\kappa_n)^{-1} \Psi_n(y), \quad y \in L', \tag{3.5}$$

and multiplication by $\Psi_m(y)$ and integration over L' gives

$$U_m^{(2)} + \kappa_m \sum_{n=0}^{\infty} k_n^{-1} \coth(k_n a)\, d_{nm} U_n^{(1)} = 0, \quad m = 1,2,\ldots. \tag{3.6}$$

Elimination of $U_m^{(2)}$ or $U_m^{(1)}$ produces equations corresponding to (2.30) and (2.32) with A_{mn}, B_{mn} replaced by A'_{mn}, B'_{mn} where

$$A'_{mn} = k_n^{-1} \coth(k_n a) \sum_{r=1}^{\infty} \kappa_r d_{mr} d_{nr}, \quad m, n = 0, 1, 2, \ldots, \tag{3.7}$$

$$B'_{mn} = \kappa_m \sum_{r=0}^{\infty} k_r^{-1} \coth(k_r a) d_{rm} d_{rn}, \quad m, n = 1, 2, \ldots. \tag{3.8}$$

We can proceed to an inhomogeneous systems of equations, as was mentioned in §2, in three different ways. The argument leading to (2.43), (2.44) can be repeated, giving an integral equation over L' and the same result is obtained if we proceed directly from (3.8). In both cases however we are expanding functions in terms of the set $\{\Psi_n(y)\}$ which is appropriate to the outer region and since there is no oscillatory term in this region a result as simple as (2.43) is not obtainable. However, if we proceed directly from (3.7), where now we are working in the inner region, we can obtain a simple result. It is convenient to redefine the unknowns $U_m^{(1)}$ by

$$k_n^{-1} \coth(k_n a) U_n^{(1)} = X_n, \quad n = 0, 1, \ldots \tag{3.9}$$

and then

$$X_m + k_m^{-1} \coth(k_m a) \sum_{n=0}^{\infty} \left(\sum_{r=1}^{\infty} \kappa_r d_{nr} d_{mr} \right) X_n = 0, \quad m = 0, 1, 2, \ldots. \tag{3.10}$$

Equations (2.30) and (3.10) are both of the form $X_m + f_m \sum_{n=0}^{\infty} g_{mn} X_n = 0$, $m = 0, 1, 2, \ldots$. If we substitute $X_m = -X_0 f_0^{-1} Y_m$ this can be rearranged to give

$$\sum_{n=0}^{\infty} \left(\sum_{r=1}^{\infty} f_r^{-1} \delta_{rm} \delta_{rn} + g_{mn} \right) Y_n = \delta_{m0}, \quad m = 0, 1, \ldots \tag{3.11}$$

and

$$Y_0 = -f_0. \tag{3.12}$$

Equations (2.43) and (2.44) then follow from (2.30), (2.31) by taking

$$f_m = k^{-1} k_m \tanh k_m a, \quad g_{mn} = k \sum_{r=1}^{\infty} \frac{c_{mr} c_{nr}}{\kappa_r},$$

and, by putting

$$f_m = k' k_m^{-1} \coth k_m a, \quad g_{mn} = k'^{-1} \sum_{r=1}^{\infty} \kappa_r d_{nr} d_{mr}$$

in (3.10), we obtain for the indentation problem

$$\sum_{n=0}^{\infty} K'_{mn} Y_n = \delta_{0m}, \quad m = 0, 1, 2, \ldots \tag{3.13}$$

and

$$Y_0 = \cot k'a, \tag{3.14}$$

where

$$K'_{mn} = \sum_{r=1}^{\infty} \{ k'^{-1} k_m \tanh(k_m a) \delta_{mr} \delta_{nr} + k'^{-1} \kappa_r d_{nr} d_{mr} \}. \tag{3.15}$$

Again it is straightforward to show that K'_{mn} is positive definite and consequently that there is an infinity of trapped-mode solutions as $a/d \to \infty$.

As for the block, only minor changes are required to set up the problem for potentials odd in x. The coth that appears in (3.5)–(3.10) is replaced by tanh, cot is replaced by $-\tan$ in (3.14) and tanh by coth in (3.15).

4. Limiting cases

For $a/d \gg 1$ it is possible to use a simple wide-spacing approximation for ϕ^s, the potential symmetric in x for the block, as follows. Above the block away from the edge $x = a$ the solution for ϕ^s will look like

$$\phi^s = A \cos kx. \tag{4.1}$$

Sufficiently close to the edge $X = 0$, where $X = x - a$, we appear to have a wave incident from $X = -\infty$ being totally reflected, since $k < \pi/2d$, with reflection coefficient R with $|R| = 1$. Thus we may write

$$\phi^s = B(\mathrm{e}^{\mathrm{i}kX} + R\,\mathrm{e}^{-\mathrm{i}kX}). \tag{4.2}$$

These two expressions are consistent provided $B = \tfrac{1}{2}A \exp(\mathrm{i}ka)$ and

$$R = \mathrm{e}^{-2\mathrm{i}ka}, \tag{4.3}$$

which provides an approximate expression for deriving the trapped-mode frequencies where R is the reflection coefficient for waves incident from $X = -\infty$ along a semi-infinite rigid block with $\phi = 0$ on $y = 0$, $X > 0$ and $k < \pi/2d$.

Of course we have no explicit expression for R except for $b = 0$ when a Wiener–Hopf solution is possible. The solution of this problem is given in Appendix A and will be used in the next section to check the accuracy of results from the full solution. For $b > 0$ a formulation similar to that used in §2 to derive (2.43), (2.44) results in

$$\sum_{n=0}^{\infty} K^{\infty}_{mn} u_n = \delta_{0m}, \quad m = 0, 1, \ldots \tag{4.4}$$

and

$$\begin{aligned} u_0 &= -\mathrm{i}(1-R)/(1+R) \\ &= \tan ka \end{aligned} \tag{4.5}$$

from (4.3), where K^{∞}_{mn} is the same as (2.45) but with $\coth k_r a$ replaced by unity.

We see therefore that the wide-spacing approximation is entirely equivalent to letting $k_r a \to \infty$, $r = 1, 2, \ldots$ in the expression for K_{mn}. For the antisymmetric solution ϕ^a and for both the symmetric and antisymmetric solutions of the indentation problem, corresponding wide-spacing approximations can be obtained by replacing the hyperbolic functions (either $\tanh k_r a$ or $\coth k_r a$) that appear in the appropriate expressions for K_{mn} by unity.

As $a/d \to 0$ we cannot expect a solution for ϕ^s if all other parameters remain fixed, since the effect of the block on motions antisymmetric in y but symmetric in x vanishes and no non-trivial solution satisfying $\phi^s \to 0$ as $x \to \infty$ is possible. This can be seen from (2.31) since $A_{mn} \to 0$ as $a/d \to 0$ whence (2.30) implies that $U^{(1)}_m = 0$ for all m. On the other hand, as we approach the cutoff frequency from below, so that $k \to \pi/2d$, we might expect unbounded solutions and this is emphasized by the term $\kappa_1^{-1} = ((\pi/2d)^2 - k^2)^{-\frac{1}{2}}$ in (2.31). Suppose now that $a/d \to 0$ and $\kappa_1 d \to 0$ *simultaneously* in such a way that $a\kappa_1^{-1}$ remains of order unity. Then the only term which remains in A_{mn} is that corresponding to $r = 1$ and we have

$$A_{mn} \to k_m^2 a\kappa_1^{-1} c_{m1} c_{n1}. \tag{4.6}$$

It follows from (2.30) that

$$U^{(1)}_m + a\kappa_1^{-1} k_m^2 c_{m1} \sum_{n=0}^{\infty} c_{n1} U^{(1)}_n = 0, \quad m = 0, 1, 2, \ldots. \tag{4.7}$$

If we multiply this by c_{m1} and sum we obtain

$$1+a\kappa_1^{-1}\sum_{n=0}^{\infty}k_n^2c_{n1}^2=0 \tag{4.8}$$

as the condition for a trapped mode. This can be written

$$\kappa_1 a^{-1}=c_{01}^2\left(k^2-\sum_{n=1}^{\infty}k_n^2(c_{n1}/c_{01})^2\right). \tag{4.9}$$

But from (B 1)

$$(c_{n1}/c_{01})^2=\tfrac{1}{8}(c/d)^4(n^2-(c/2d)^2)^{-2},\quad n\geqslant 1,$$

whilst

$$c_{01}^2=8(d/c)\pi^{-2}\cos^2(\tfrac{1}{2}\pi b/d).$$

Equation (4.9) can therefore be written

$$\frac{\kappa_1 d}{(a/d)}=\frac{8\cos^2(\frac{1}{2}\pi b/d)}{\pi^2c/d}\left(\frac{\pi^2}{4}-\frac{\pi^2c^2}{8d^2}\sum_{n=1}^{\infty}\frac{1}{n^2-c^2/4d^2}+O(\kappa_1^2d^2)\right). \tag{4.10}$$

Using the result

$$\sum_{n=1}^{\infty}\frac{1}{n^2-A^2}=\frac{1}{2A^2}-\frac{\pi}{2A}\cot\pi A$$

this reduces to

$$(\kappa_1 d)/(a/d)=\tfrac{1}{2}\pi\sin(\pi b/d) \tag{4.11}$$

in this simultaneous limit.

It can be seen that this simple approximation is not valid when $b=0$, corresponding to a thin strip of length $2a$ on the centreline $y=0$. Equation (4.11) corresponds to a trapped-mode frequency given by

$$kd=\tfrac{1}{2}\pi(1-\tfrac{1}{2}(a/d)^2\sin^2(\pi b/d)). \tag{4.12}$$

The above argument does not hold for the solution ϕ^{a}, since the limit $a/d\to 0$ with $\kappa_1 d$ *fixed* no longer implies $\phi^{\mathrm{a}}=0$ since the effect of the block on solutions odd in y *and* odd in x does not vanish as $a/d\to 0$. Thus it is not possible to combine this limit with the unboundedness of ϕ^{a} as $\kappa_1\to 0$ simultaneously. This can be seen from the expression corresponding to (2.31) in the ϕ^{a} problem since A_{mn} does not obviously tend to a limit as a/d, $\kappa_1 d\to 0$ simultaneously.

We can however consider this limit for the solutions to the indentation problem symmetric in x. The condition for a trapped mode, equivalent to equation (4.8), is now

$$1+a^{-1}\kappa_1\sum_{n=0}^{\infty}k_n^{-2}d_{n1}^2=0. \tag{4.13}$$

Substituting for d_{n1} from (B 2) gives

$$\frac{a/d}{\kappa_1 d}\approx\frac{4}{\pi^4}\left\{\frac{16\cos^2(\pi d/2b)}{(1-(d/b)^2)^3}-\sum_{n=1}^{\infty}\frac{(n+\frac{1}{2})^2\cos^2[(n+\frac{1}{2})\pi d/b]}{((n-\frac{1}{2})^2(d/b)^2-\frac{1}{4})^3}\right\}, \tag{4.14}$$

and again this approximation is not valid when $b=0$.

In both the block problem and the indentation problem there is an additional limit which should give rise to a trapped-mode condition. Thus, for the block, if $b/d\to 1$, $\kappa_1 d$ fixed, the block completely fills the channel, $\phi\to 0$ and there is no trapped mode. If however $b/d\to 1$ and $\kappa_1 d\to 0$ simultaneously we might expect to obtain a trapped-mode condition. Careful consideration of (2.31) together with (B 3) shows that in this limit all the coefficients A_{mn} vanish except for A_{00}, provided $(c/d)/(\kappa_1 d)$ is of order unity. Thus in this simultaneous limit

$$1-2(c/d)\,k\tan(ka)(\kappa_1 d)^{-1} = 0. \tag{4.15}$$

This corresponds to a trapped-mode frequency given by the roots of the equation

$$kd = \tfrac{1}{2}\pi(1-2(c/d)^2\tan^2 ka). \tag{4.16}$$

The corresponding approximation for the antisymmetric problem is obtained by replacing the $\tan^2 ka$ in (4.16) by $\cot^2 ka$. In the indentation problem with $b/d \rightarrow 1$ and $\kappa_1 d \rightarrow 0$ simultaneously we have both $k_0 d = \mathrm{i}k'd = \mathrm{i}(k^2-p_0^2)^{\frac{1}{2}}d$ and $\kappa_1 d = (l_1^2-k^2)^{\frac{1}{2}}d$ small and so, from (3.10),

$$1-\frac{\kappa_1}{k'^2 a}d_{01}^2 = 0 \tag{4.17}$$

provided $\kappa_1/k'^2 a$ is of order unity. From (B 4) we have $d_{01}^2 \rightarrow 1$ as $b/d \rightarrow 1$, whence

$$\kappa_1 = k'^2 a \tag{4.18}$$

in this simultaneous limit. Equation (4.18) corresponds to a trapped-mode frequency given by

$$kd = \tfrac{1}{2}\pi(1-\tfrac{1}{2}\pi^2(ca/db)^2). \tag{4.19}$$

No simple limiting conditions in the cases $a/d \rightarrow 0$, $\kappa_1 d \rightarrow 0$ or $k'd \rightarrow 0$, $\kappa_1 d \rightarrow 0$ appear to exist for the antisymmetric solution to the indentation problem.

5. Results

We shall begin by discussing the numerical procedures used with reference to the symmetric solution, ϕ^s, for the block. The two formulations that were used to solve the problem give rise to two methods for computing the trapped-mode frequencies.

The first method uses (2.30) with A_{mn} given by (2.31). In order for there to be a non-trivial solution of (2.30) we require

$$\det(\boldsymbol{I}+\boldsymbol{A}) = 0, \tag{5.1}$$

where $\boldsymbol{A}$ is the infinite matrix with elements A_{mn}. To find these zeros numerically we truncate the system (2.30) to an $N\times N$ system and find values of kd such that

$$\det(\boldsymbol{I}^{(N)}+\boldsymbol{A}^{(N)}) = 0. \tag{5.2}$$

In order to achieve convergence of the determinant as N increases it is necessary to scale the matrix $\boldsymbol{I}^{(N)}+\boldsymbol{A}^{(N)}$ by its diagonal elements. Thus we compute the zeros of $\det(\boldsymbol{M}^{(N)})$ where the elements of $\boldsymbol{M}^{(N)}$ are $(\delta_{mn}+A_{mn})/(1+A_{mm})$, $m, n \leqslant N$. The simple one-term approximation given by (2.34) corresponds to $1+A_{00} = 0$ and thus to an infinity of $\det(\boldsymbol{M}^{(N)})$. As an example figure 2 shows the behaviour of $\det(\boldsymbol{M}^{(N)})$ as a function of kd for the parameter values $a/d = b/d = \frac{1}{2}$ and we can see that (2.34) provides a good approximation to the actual solution. The value of N used was $N =$ 40 and tests suggest that with this truncation parameter results are accurate to within about 1%. This point will be discussed again later with reference to the exact solution corresponding to $b = 0$. It should be noted that the summation involved in calculating A_{mn} from (2.31) converges fairly slowly. It is important that the summation is continued well beyond $r = \max\{m, n\}/(1-b/d)$ since the denominator becomes small there. In practice $20N$ terms of this sum were used and, except for

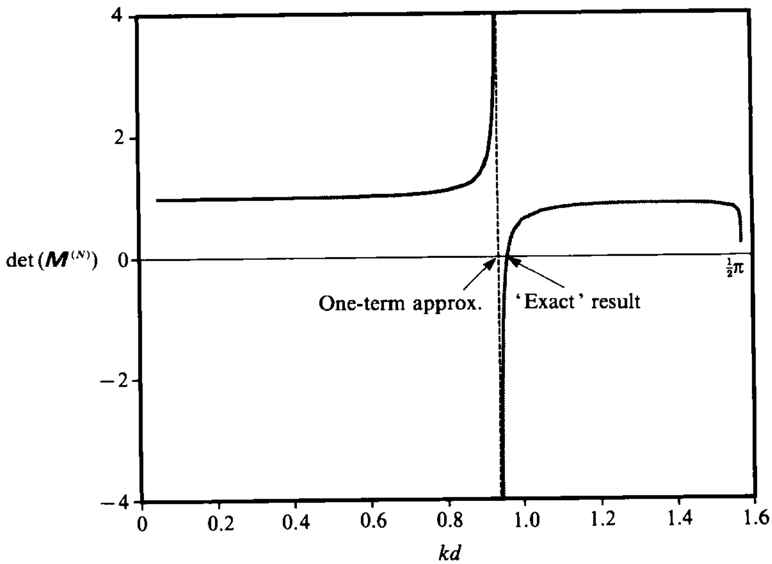

FIGURE 2. Variation of det $(\boldsymbol{M}^{(N)})$ with kd when $a/d = b/d = 0.5$, $N = 40$.

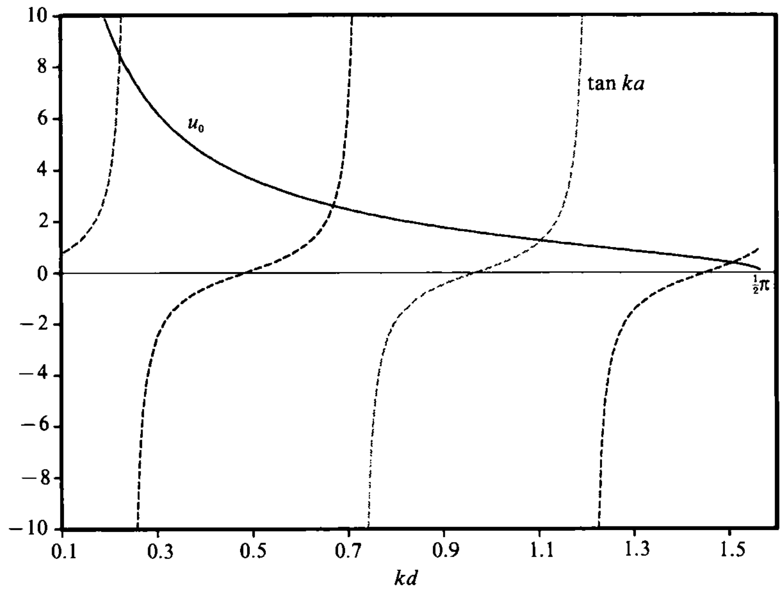

FIGURE 3. Curves of u_0 and $\tan ka$ plotted against kd for $a/d = 6.5$, $b/d = 0.5$.

values of b/d very close to one, it was found that the errors introduced by this truncation were an order of magnitude smaller than those introduced by the initial $N \times N$ truncation.

For large values of a/d we expect to get more than one solution to det $(\boldsymbol{M}^{(N)}) = 0$ owing to the periodicity of $\tan ka$ which appears in A_{00}. It is more instructive to consider the second formulation, (2.43), (2.44), in order to see where these other roots lie. Figure 3 shows a curve of u_0, found by solving (2.43), against kd. Plotted on the same figure is the graph of $\tan ka$ so that the intersections represent the trapped-mode values. Here $a/d = 6.5$, $b/d = 0.5$ and $N = 40$.

$20kd/\pi$	$\beta+\frac{1}{2}\pi$	$\tan^{-1}[(K^{\infty})^{-1}_{00}], N = 40$
1	1.5013	1.5010
2	1.4310	1.4304
3	1.3586	1.3577
4	1.2831	1.2819
5	1.2028	1.2013
6	1.1151	1.1134
7	1.0162	1.0142
8	0.8982	0.8958
9	0.7406	0.7380

TABLE 1

a/d	Full solution $N = 40$	Small a/d, equation (4.12)	Large a/d $N = 40$
0.05	1.569	1.570	
0.1	1.563	1.567	1.568
0.2	1.531	1.555	1.536
0.4	1.402	1.508	1.404
0.6	1.243		1.244
0.8	1.097		1.097
1.0	0.974		0.974

TABLE 2

In practice the following method was used to compute the trapped-mode frequencies. First the inhomogeneous system was solved with a small truncation size to show where and how many roots there were and then the one-term approximation equivalent to (2.34) was used to compute approximate roots which provided initial guesses for determining the roots more accurately, either by finding the zeros of $\det(\boldsymbol{M}^{(N)})$ or of $(K^{(N)})^{-1}_{00} - \tan ka$. Here $(K^{(N)})^{-1}_{mn}$ refers to the (m, n) element of the inverse of $\boldsymbol{K}^{(N)}$.

Before looking at the actual trapped-mode frequencies that are obtained let us compare answers obtained from the full solution with $b = 0$ with those obtained from the Wiener–Hopf solution given in Appendix A. Thus from (A 14), (4.3) and (4.4) we should have

$$-\cot\beta = (K^{\infty})^{-1}_{00} \tag{5.3}$$

or

$$\beta + \tfrac{1}{2}\pi = \tan^{-1}[(K^{\infty})^{-1}_{00}] + n\pi$$

for some integer n, and where β is given by (A 15). Table 1 shows, with $n = 0$, the accuracy obtained by using a truncation size of 40 when evaluating $(\boldsymbol{K}^{\infty})^{-1}$. The sum in (A 15) can be computed very accurately with little effort and the results shown in the table are accurate to four decimal places.

These results give us confidence in those results which cannot be compared with such exact formulae.

We shall now examine the accuracy of the small- a/d and large- a/d approximations discussed in §4. Table 2 shows the trapped-mode frequencies that are obtained by three different means. Column 2 contains the results from the full solution whilst column 3 was computed using the small-a/d result (4.12) and column 4 was computed from the large-a/d result obtained by replacing the coth $k_r a$ that appears in (2.45) by unity. In this example $b/d = 0.25$.

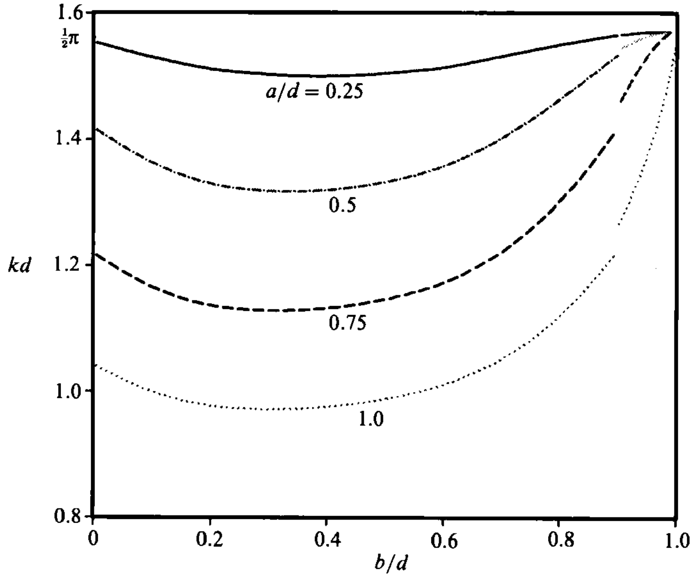

FIGURE 4. Variation with b/d of symmetric trapped-mode frequencies of a block, for four values of a/d. Equation (4.16) was used for values of b/d greater than 0.9.

It is clear that the small-a/d result given by equation (4.12) only predicts trapped-mode frequencies to within 1% when a/d is less than about 0.1. On the other hand the large-a/d approximation agrees with the full solution to within 1% for all a/d greater than about 0.1. An estimate of the error involved in replacing $\coth k_r a$ in (2.45) by unity can be made as follows. It is sufficient to consider the case $r = 1$ when it can be shown that the inequality $\coth k_r a - 1 < f/100$ implies $a/d > \frac{1}{2}(k_1 d)^{-1} \times \ln(200/f+1)$. But $(k_1 d)^{-1} = \pi^{-1}(c/d)(1-(kc/\pi)^2)^{-\frac{1}{2}}$, so that $\max(k_1 d)^{-1} = 2/(3^{\frac{1}{2}}\pi)$, obtained when both $c/d = 1$ and $kd = \frac{1}{2}\pi$. Thus $a/d > 3^{-\frac{1}{2}}\pi^{-1}\ln(200/f+1)$ ensures f% accuracy for all c/d and whatever the eventual value of kd. For example, an error of less than 1% (5%) is ensured for all c/d if $a/d > 0.97$ (0.68), and for $c/d = \frac{1}{2}$, if $a/d > 0.42$ (0.30).

It should be noted that computation of $(\boldsymbol{K}^{\infty})^{-1}$ is as time consuming as computing $\boldsymbol{K}^{-1}$. However there are a number of advantages in using this large a/d approximation. For example $(\boldsymbol{K}^{\infty})^{-1}$ is independent of a/d so that only one matrix inversion is necessary when computing solutions over a range of values of a/d. Notice also that the form of $\boldsymbol{K}^{\infty}$ is the same when we consider motions antisymmetric in x and so the curve of u_0 shown in figure 3 is equally applicable to antisymmetric modes (except for very small a/d). But now these modes correspond to the intersection of the u_0 curve with that of $-\cot ka$. Since $-\cot ka$ is negative for $0 < ka < \frac{1}{2}\pi$ we see that there are no roots for $ka < \frac{1}{2}\pi$ and so any difference between the symmetric and antisymmetric curves for u_0 when a/d is small is irrelevant when computing antisymmetric trapped modes.

Returning to the solution for ϕ^s, figure 4 shows how the trapped-mode frequencies vary as b/d varies between 0 and 1 for four different values of a/d. For values of b/d greater than 0.9 the exact curves are replaced by approximate solutions computed from (4.16). We can see that all the curves tend to $\frac{1}{2}\pi$ as $b/d \to 1$ but that this convergence is very slow and over most of the range of b/d, except for $b/d \approx 1$, the sensitivity of the trapped-mode frequencies to variations in b/d is small.

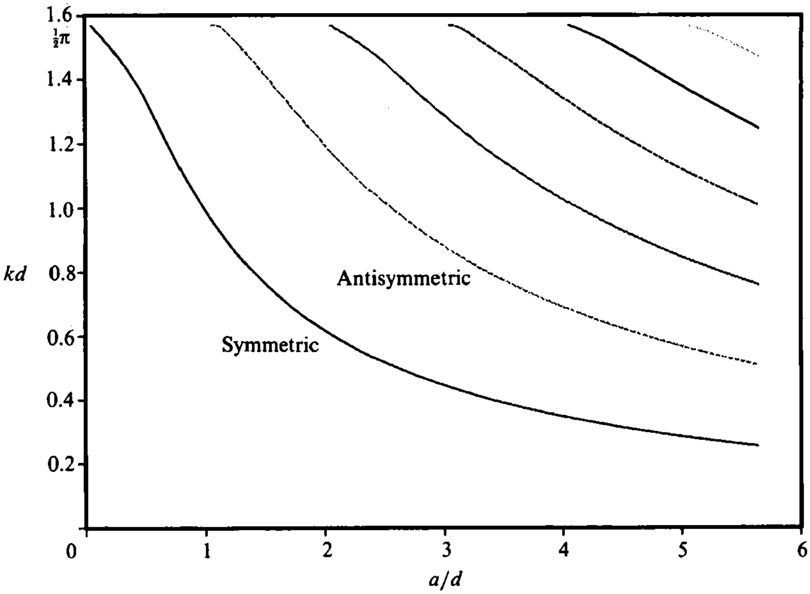

FIGURE 5. Variation with a/d of trapped-mode frequencies of a block when $b/d = 0.5$.

Notice that for all the values of a/d plotted in figure 4 there is just one trapped-mode frequency. Figure 5 shows how the trapped-mode frequencies vary as a/d varies and in the light of the remark made in the previous paragraph about the insensitivity of the results to the value of b/d, only one value of b/d is used, namely $b/d = 0.5$. The figure shows both the solutions for the symmetric modes and those for the antisymmetric modes. We can see that there are m symmetric trapped-mode frequencies whenever $2(m-1) < a/d \leqslant 2m$ and that there are m antisymmetric trapped-mode frequencies whenever $2m-1 < a/d \leqslant 2m+1$. Thus there are m trapped-mode frequencies in total whenever $m-1 < a/d \leqslant m$.

The insensitivity of $\boldsymbol{K}$ to variations in a/d also provides further insight into the disposition of the trapped modes as a/d varies for fixed kd. Thus from (2.43), (2.44) u_0 is effectively independent of a/d, for a/d not too small, and it follows that for *fixed* kd, values of a/d at which successive trapped modes occur are spaced $\pi/2kd$ apart to a high accuracy. This is borne out by the numerical results and by figure 5.

We will now turn our attention to the indentation problem. Figure 6 shows a curve of u_0, computed using (3.13), together with the curves of $\cot k'a$ and $-\tan k'a$ plotted against kd. Here we are restricted to the region $\pi d/2b < kd < \frac{1}{2}\pi$. The intersections of the u_0-curve with the curve of $\cot k'a$ thus correspond to the trapped-mode frequencies for the symmetric problem. Again, computations show that replacing the $\tanh k_m a$ in (3.15) by unity or $\coth k_m a$ does not affect the curve of u_0 appreciably except when a/d is very small, and so the solutions to the antisymmetric problem for $a/d = 6.5$ are given to good accuracy by the intersection of the same curve for u_0 with the curve of $-\tan k'a$. For the block with large a/d the trapped-mode frequencies were fairly evenly spaced along the kd-axis but in this case, owing to the nonlinear relationship between k and k', this is not so and the solutions are closer together near $kd = \frac{1}{2}\pi d/b$.

The variation of the trapped-mode frequencies with the depth of indentation is shown in figure 7 for four different values of a/d. It can be seen that the variation

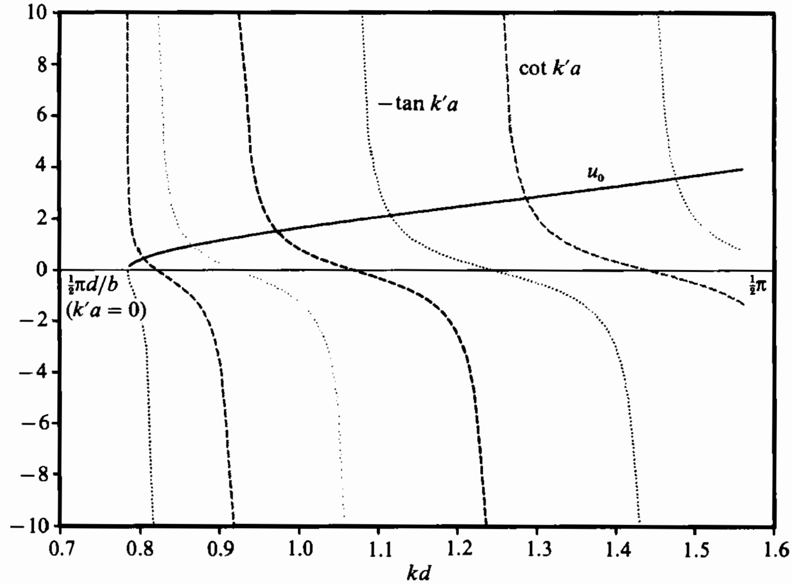

FIGURE 6. Curve of u_0, computed from (3.13), plotted against kd, $a/d = 6.5$, $d/b = 0.5$. The intersections with the curve of $\cot k'a$ are the symmetric trapped-mode frequencies whilst the antisymmetric trapped-mode frequencies come from the intersections with the curve of $-\tan k'a$.

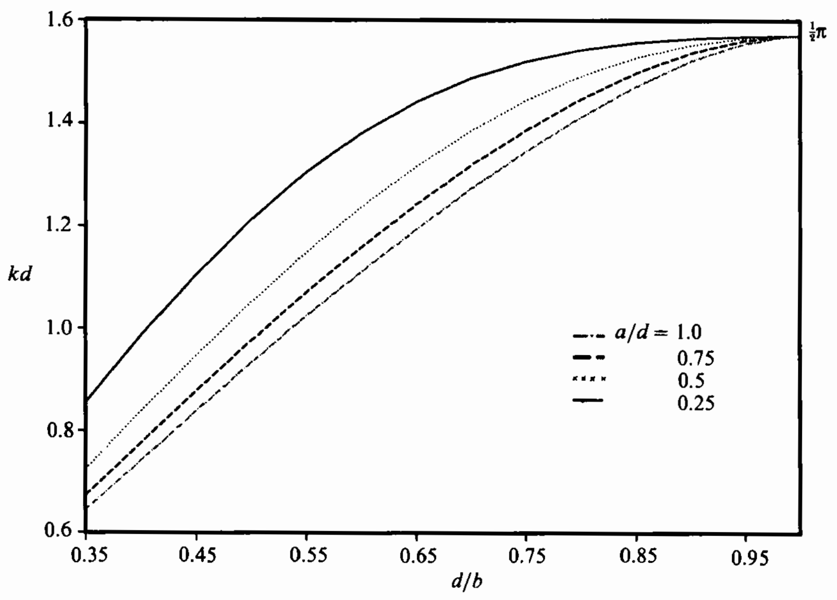

FIGURE 7. The variation of trapped-mode frequencies with the depth of indentation of four values of a/d.

with d/b is greater than in the case of the block and that the convergence of the trapped-mode frequencies to $\frac{1}{2}\pi$ as $d/b \to 1$ is more rapid. The curves also demonstrate the validity of (4.19) when d/b is close to unity, since this formula was used to compute the curves shown for values of d/b greater than 0.95.

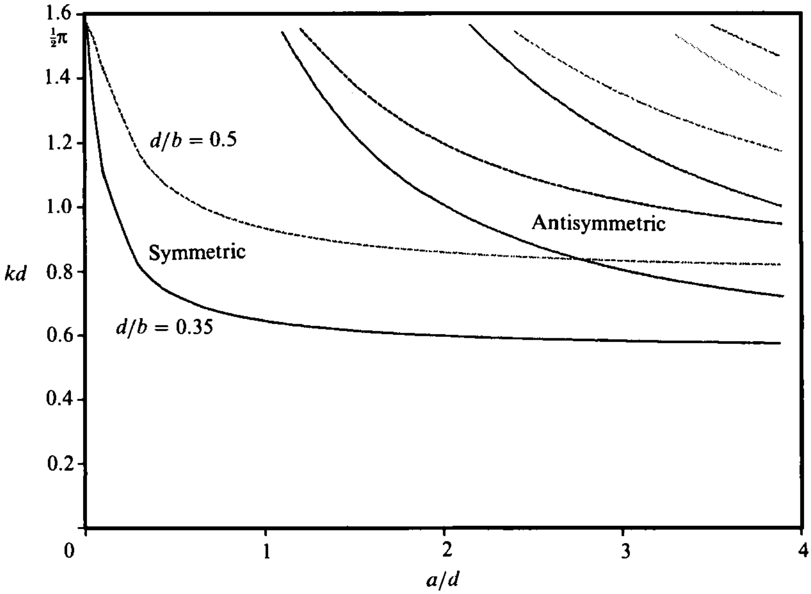

FIGURE 8. Variation with a/d of trapped-mode frequencies for an indentation.

Finally figure 8 shows the variation of both the symmetric and antisymmetric trapped-mode frequencies with a/d for two values of d/b, namely $d/b = 0.35$ and 0.5. The curves show that as a/d becomes large the first (symmetric) trapped mode approaches the lower cutoff, $kd = \frac{1}{2}\pi d/b$, fairly rapidly. The condition for m trapped modes is now $m-1 < a/d(1-d/b)^{\frac{1}{2}} < m$.

6. Trapped acoustic waves

In the previous sections we have considered trapped water waves in an infinitely long channel containing either a symmetrically placed rectangular block immersed throughout the depth, or a symmetric rectangular indentation in each wall. In every case we have had to seek solutions which are antisymmetric with respect to the centreline of the channel in order to allow for the possibility of trapped-wave frequencies below the cutoff frequency or $k < \pi/2d$.

As mentioned in the introduction the equations describe equally well the linearized equations of acoustics in a parallel-plate wave guide containing a rectangular obstacle or indentation.

Released from the physical requirements of the water-wave problem we can consider different boundary conditions in the acoustic case corresponding to 'soft' or 'hard' boundary conditions or a combination of both. For example, if in the indentation problem of §3 we apply the 'soft' condition on *all* boundaries as well as the centreline $y = 0$, the appropriate orthogonal functions in regions I and II are $\sin p_n y$ and $\sin l_n y$ respectively, where $p_n = n\pi/b$, $l_n = n\pi/d$, $n = 1, 2, \ldots$. We can now anticipate trapped modes for values of k satisfying $\pi/b < k < \pi/d$. This problem is of a type covered by Jones (1953) and application of his theorem $3a$ implies that there are at least P trapped modes, where P is the number of eigenvalues $\mu_{mn} \equiv ((n\pi/a)^2 + (m\pi/b)^2)^{\frac{1}{2}}$, $m, n = 1, 2, \ldots$ which are less than π/d. Thus if $a^{-2} + b^{-2} < d^{-2}$ at least one trapped mode exists. Application of our theory described in §3 to this case suggests that there is in fact at least one trapped mode if $a^{-2}+b^{-2} < 2d^{-2}$ and thus that the bounds given by Jones might be improved upon as was noticed by Evans & McIver (1984) when looking at edge waves over a shelf. Jones' result also demonstrates that provided $b > d$ the number of trapped modes that exist tends to infinity as $a/d \rightarrow \infty$, which is also confirmed by the present theory. Another example arises if the soft condition on $y = 0$ is replaced by the hard condition $\phi_y = 0$ whilst retaining the condition $\phi = 0$ on the other boundaries: the modes in I, II are $\cos p_n y$ and $\cos l_n y$ with $p_n = (n+\frac{1}{2})\pi/b$, $l_n = (n+\frac{1}{2})\pi/d$, $n = 0, 1, \ldots$ and trapped modes can be expected for $\frac{1}{2}\pi/b < k < \frac{1}{2}\pi/d$.

These examples by no means exhaust the possibilities for trapped modes. What is required in general is that the lowest mode in the finite inner region I be less than the lowest mode in the infinite outer region II so that a trapped mode having a value of k lying between them can be sought. This will ensure that the general solution decays as $|x| \rightarrow \infty$ whilst at the same time allowing an oscillatory first term in the region I. Further development of these ideas to three-dimensional acoustic waves in wave guides of arbitrary cylindrical cross-section is in preparation.

7. Conclusion

A numerical scheme has been developed for the determination of trapped-mode frequencies which appear to exist below the first cutoff frequency in a wave tank containing a symmetrically placed rectangular rigid block extending throughout the water depth. The modes, which are antisymmetric about the centreline of the channel, may be either symmetric or antisymmetric about a line through the middle of the block perpendicular to the channel walls. The modes appear to exist for all dimensions of the block including $b = 0$ when it reduces to a thin plate on the centreline of the channel. As the length a along the channel increases with b/d fixed, additional modes occur.

Similar methods have been used to predict the trapped-mode frequencies in the presence of a symmetric rectangular indentation in the walls of the wave tank. Again the modes are antisymmetric about the centreline but may be symmetric or antisymmetric with respect to a line through the middle of the indentation perpendicular to the channel walls.

Explicit approximate expressions for the determination of the trapped-mode frequencies have been derived in certain limiting cases but in general the solution required the inversion of an infinite system of equations.

It is believed that the existence of these particular trapped modes has not been noticed hitherto and it should be emphasized that the present method does not constitute a rigorous proof. However, Jones (1953) has proved the existence of point-eigenvalues corresponding to trapped modes in a related and more general context but which does not appear to include the problems considered in detail here, although it is entirely possible that his method could be adapted to cover these problems also. Again, more recently, both M. Callan and P. McIver (1990, personal communications) have verified the existence of trapped modes in the presence of a small vertical circular cylinder placed symmetrically in the wave tank, or equivalent acoustic wave guide.

Although the method used in this paper only applies to rectangular geometries there appears to be little doubt that trapped modes can exist in a wide variety of wave-guide problems provided a cutoff frequency exists. Further work in this area is under way.

D.V.E. would like to thank Professor Fritz Ursell for a useful discussion which prompted the present work, whilst C.M.L. acknowledges the support of SERC MTD Ltd under grant number GR/F/32226.

Appendix A

We seek $\phi(x,y)$ satisfying

$$(\nabla^2+k^2)\phi = 0, \quad 0 \leqslant y \leqslant d, \quad \text{all } x, \tag{A 1}$$

$$\phi_y = 0, \quad \begin{cases} y = d, & -\infty < x < \infty, & \text{(A 2)} \\ y = 0, & x < 0, & \text{(A 3)} \end{cases}$$

$$\phi = 0, \quad y = 0, \quad x > 0, \tag{A 4}$$

$$\phi \to 0, \quad x \to +\infty, \tag{A 5}$$

$$\phi \sim \mathrm{e}^{\mathrm{i}kx} + R\,\mathrm{e}^{-\mathrm{i}kx}, \quad x \to -\infty, \tag{A 6}$$

and in particular we seek R, for $k < \frac{1}{2}\pi/d$. Standard Wiener–Hopf theory can be used to show that

$$\phi(x,y) = \mathrm{e}^{\mathrm{i}kx} + \frac{\mathrm{i}kd}{\pi}\int_C \mathrm{e}^{-\mathrm{i}\alpha x} K_-(-k)\,K_+(\alpha)\,\frac{\cosh\gamma(d-y)\,\mathrm{d}\alpha}{\gamma\sinh\gamma d}, \tag{A 7}$$

where $\gamma^2 = \alpha^2 - k^2$, C is a path along the real α-axis indented to pass above the pole at $\alpha = -k$ and below that at $\alpha = +k$, and

$$K_+(\alpha)\,K_-(\alpha) = (\tanh\gamma d)/\gamma d, \tag{A 8}$$

where $K_\pm$ is regular in $\mathscr{D}_\pm : \operatorname{Im}\alpha \gtrless 0$.

Clearly (A 7) satisfies (A 1), (A 2). The condition (A 3) follows from differentiation and the regularity of $K_+(\alpha)$ in $\mathscr{D}_+$. To confirm (A 4) we use (A 8) and deform the contour C into $\mathscr{D}_-$ where now the integrand is regular apart from a contribution from the pole at $\alpha = -k$ which cancels the term $\mathrm{e}^{\mathrm{i}kx}$.

For $x \lessgtr 0$ we may deform C into $\mathscr{D}_\pm$ to show

$$\phi(x,y) = \mathrm{e}^{\mathrm{i}kx} + K_+(k)\,K_-(-k)\,\mathrm{e}^{-\mathrm{i}kx} + O(\exp(k_n x)), \quad x < 0 \tag{A 9}$$

and

$$\phi(x,y) = 0\,(\exp(-\kappa_n x)), \quad x > 0, \tag{A 10}$$

confirming (A 5) and (A 6).

So

$$R = -K_+(k)\,K_-(-k). \tag{A 11}$$

Now it can be shown that

$$K_+(\alpha) = \prod_{n=1}^{\infty}\left(\frac{k_n - \mathrm{i}\alpha}{\kappa_n - \mathrm{i}\alpha}\right)\frac{l_n}{p_n} = K_-(-\alpha), \tag{A 12}$$

so that

$$R = -(K_+(k))^2$$

$$= -\prod_{n=1}^{\infty}\left(\frac{k_n - \mathrm{i}k}{\kappa_n - \mathrm{i}k}\right)^2 \frac{l_n^2}{p_n^2} \tag{A 13}$$

$$= -\exp(-2\mathrm{i}\beta), \tag{A 14}$$

where
$$\beta = \sum_{n=1}^{\infty} \left(\tan^{-1}\left(\frac{k}{k_n}\right) - \tan^{-1}\left(\frac{k}{\kappa_n}\right)\right) \tag{A 15}$$
after some reduction.

Appendix B

We require for the rectangular block, with $c = d-b$,

$$c_{mn} = \int_b^d \psi_m(y)\, \Psi_n(y)\, \mathrm{d}y = \left(\frac{2\epsilon_m}{dc}\right)^{\frac{1}{2}} \int_b^d \cos\frac{m\pi}{c}(d-y) \sin(n-\tfrac{1}{2})\frac{\pi y}{d}\,\mathrm{d}y$$
$$= \begin{cases} \left(\dfrac{2\epsilon_m d}{c}\right)^{\frac{1}{2}} \dfrac{(-1)^m (n-\frac{1}{2}) \cos(n-\frac{1}{2})\pi b/d}{\pi[(n-\frac{1}{2})^2 - m^2 d^2 c^{-2}]}, & n-\frac{1}{2} \neq dm/c \\ \left(\dfrac{\epsilon_m c}{2d}\right)^{\frac{1}{2}} (-1)^{n+1}\left(1+\dfrac{\sin 2m\pi b/c}{2m\pi}\right), & n-\frac{1}{2} = dm/c, \end{cases} \tag{B 1}$$

whilst for the indentation

$$d_{mn} = \int_0^d \psi'_m(y)\, \Psi_n(y)\, \mathrm{d}y = 2(bd)^{-\frac{1}{2}} \int_0^d \sin(m+\tfrac{1}{2})\frac{\pi y}{b} \sin(n-\tfrac{1}{2})\frac{\pi y}{d}\,\mathrm{d}y$$
$$= \begin{cases} 2\left(\dfrac{d}{b}\right)^{\frac{3}{2}} \dfrac{(-1)^n (m+\frac{1}{2}) \cos(m+\frac{1}{2})\pi d/b}{\pi[(m+\frac{1}{2})^2 d^2 b^{-2} - (n-\frac{1}{2})^2]}, & (n-\frac{1}{2})b \neq m+\frac{1}{2} \\ (d/b)^{\frac{1}{2}}, & (n-\frac{1}{2})b = m+\frac{1}{2}. \end{cases} \tag{B 2}$$

The special cases $n-\frac{1}{2} = dm/c$ in (B 1) and $(n-\frac{1}{2})b = m+\frac{1}{2}$ in (B 2) are not of any practical importance since b, and hence c, can be chosen so that they cannot be expressed as a fraction of the form $m/(n-\frac{1}{2})$ (or $(m+\frac{1}{2})/(n-\frac{1}{2})$) for $m, n < N$, the truncation size. The quantities c_{mn} and d_{mn} are well behaved near these points owing to the vanishing of the cosine term in the numerator.

We also require the limits of these functions as $b/d \rightarrow 1$ or equivalently as $c/d \rightarrow 0$. Thus

$$\left.\begin{aligned} c_{mn} &\rightarrow 2(c/d)^{\frac{5}{2}}(-1)^{n+m}\frac{(n-\frac{1}{2})^2}{m^2}, & m \geqslant 1 \\ &\rightarrow 2^{\frac{1}{2}}(c/d)^{\frac{1}{2}}(-1)^{n+m+1}, & m = 0 \end{aligned}\right\} \text{ as } c/d \rightarrow 0 \tag{B 3}$$

and

$$\left.\begin{aligned} d_{mn} &\rightarrow (c/d)\frac{2(-1)^{n+m+1}(m+\frac{1}{2})^2}{[(m+\frac{1}{2})^2-(n-\frac{1}{2})^2]}, & n \neq m+1 \\ &\rightarrow (-1)^{n+m+1} & n = m+1 \end{aligned}\right\} \text{ as } c/d \rightarrow 0. \tag{B 4}$$

REFERENCES

EVANS, D. V. & MCIVER, P. 1984 Edge waves over a shelf: full linear theory. *J. Fluid Mech.* **142**, 79–95.

JONES, D. S. 1953 The eigenvalues of $\nabla^2 u + \lambda u = 0$ when the boundary conditions are given on semi-infinite domains. *Proc. Camb. Phil. Soc.* **49**, 668–684.

LEBLOND, P. H. & MYSAK, L. A. 1978 *Waves in the Ocean*. Elsevier.

MCIVER, P. & EVANS, D. V. 1985 The trapping of surface waves above a submerged horizontal cylinder. *J. Fluid Mech.* **151**, 243–255.

NOBLE, B. 1958 *Methods based on the Wiener–Hopf Technique for the Solution of Partial Differential Equations*. Pergamon.

RAZAVY, M. 1989 An acoustic waveguide with variable cross section. *J. Acoust. Soc. Am.* **86**, 1155–1160.

STOKES, G. G. 1846 Report on recent researches in hydrodynamics. *Brit. Assoc. Rep.*

URSELL, F. 1951 Trapping modes in the theory of surface waves. *Proc. Camb. Phil. Soc.* **47**, 347–358.

URSELL, F. 1952 Edge waves over a sloping beach. *Proc. R. Soc. Lond.* A **214**, 79–97.

URSELL, F. 1987 Mathematical aspects of trapping modes in the theory of surface waves. *J. Fluid Mech.* **183**, 421–437.